Effects of polypropylene fibre type and dose on the propensity for heat-induced concrete spalling

Effects of Polypropylene Fibre Type and Dose on the Propensity for Heat-Induced Concrete Spalling

Cristian Maluk[1,*], Luke Bisby[1], and Giovanni P Terrasi[2]

[1] School of Engineering, The University of Edinburgh, UK

[2] Empa, Swiss Federal Laboratories for Material Science and Technology, Switzerland

Abstract

The term *high-performance* concrete (HPC) is typically used to describe concrete mixes with high workability, strength, and/or durability. While HPC outperforms normal strength concrete in nearly all performance criteria, it also displays a higher propensity for heat-induced concrete spalling when exposed to severe heating or fire. Such spalling presents a serious concern in the context of the historical approach to fire safe design of concrete structures, where structural engineers typically rely on concrete's inherent fire safety characteristics (e.g. non-combustibility, non-flammability, high thermal inertia). It has been widely shown that the inclusion of polypropylene (PP) fibres in concrete mixes reduces the propensity for heat-induced concrete spalling, although considerable disagreement exists around the mechanisms behind the fibres' effectiveness. This paper presents an experimental study on the effects of PP fibre type and dose on the propensity for heat-induced spalling of concrete. A novel testing method and apparatus, the Heat-Transfer Rate Inducing System (H-TRIS) is used to test medium-scale concrete specimens under simulated standard fire exposures. Results show (1) that although the dose of PP fibres (mass of PP per m^3 of fresh concrete) is currently the sole parameter prescribed by available design guidelines, both the PP fibre cross-section and individual fibre length may have considerable influences on the effectiveness of PP fibres at reducing the propensity for heat-induced concrete spalling; and (2) that current guidance for spalling mitigation with PP fibres is insufficient to prevent spalling for the HPC mixes tested.

Keywords

Heat-induced concrete spalling; high-performance concrete; polypropylene fibres; fire testing; H-TRIS.

---

[*] **Corresponding Author**

Currently at: School of Civil Engineering, The University of Queensland, Australia

Address: School of Civil Engineering, The University of Queensland, Brisbane QLD 4072, Australia

Email: c.maluk@uq.edu.au

Tel: +61 7 3365 3518

1 INTRODUCTION & BACKGROUND

Structural engineers have historically relied on concrete's inherent fire safety characteristics (e.g. non-combustibility, non-flammability, high thermal inertia) for the fire safe design of concrete structures [1]. Modern advances in concrete construction have been driven by the need to build faster and higher, to reduce cost, increase sustainability, and increase service lives. The term *high-performance* concrete (HPC) describes concrete mixes with high workability, strength, and durability, and low compressive creep [2, 3].

While HPC outperforms normal concrete in nearly all performance criteria, *"its Achilles heel is its performance when exposed to fire"* [4]; it has a high propensity for explosive spalling under severe heating and also experiences more rapid reductions in compressive strength than 'normal' strength concrete at elevated temperature [5]. Given its ever-increasing use in high-rise buildings (particularly for columns), and in tunnel structures and lining segments [6], the heat-induced spalling resistance of HPC is a critical issue for the concrete industry (in-situ and precast).

1.1 Spalling

Heat-induced spalling of concrete, which is widely perceived as being a random phenomenon [7], occurs when the exposed surface of heated concrete flakes away in a more or less violent manner (see Figure 1). As a consequence, the concrete cover to the internal reinforcement is reduced, resulting in more rapid temperature increases of the internal reinforcement and within the core of the structural element, in addition to a direct influence on load bearing capacity due to the loss of physical or effective cross sectional area. Heat-induced concrete spalling presents a potentially serious concern in the context of the historical approach to fire safe structural design of concrete structures, where spalling is less common and presumed as

53 ‘implicitly’ accounted for in prescriptive, tabulated fire design guidance. The concrete
54 industry is beginning to grapple with the implications of the clearly demonstrated increased
55 propensity for spalling of modern high-performance concrete mixes [7, 8] and its possible
56 effects on the fire resistance of concrete structures.

57
58 **Figure 1 – Evidence of the significant extent of spalling on the soffit of a large-scale concrete specimen**
59 **after a standard fire resistance test (photo courtesy Ieuan Rickard).**

60 Heat-induced concrete spalling is by no means a new phenomenon (e.g. [9] to [18]), although
61 as noted it is increasingly a concern for modern HPC mixes. Numerous past researchers have
62 studied heat-induced concrete spalling, mainly focusing their efforts on:

63 • understanding the thermo-physical mechanisms leading to spalling, thus studying the
64 factors which influence its occurrence [11, 12, 17, 18, 19];

65 • modelling (analytically or numerically) the occurrence of spalling [20, 21];

66 • modelling of the potential impacts of spalling on the load bearing capacity of structural
67 systems [22, 23]; and

68 • defining techniques to diminish and/or avoid the occurrence of spalling [13, 24].

1.2 Polypropylene fibres

More than three decades of experimental studies have convincingly shown that polypropylene (PP) fibres' (see Figure 2) inclusion in fresh concrete can considerably reduce the propensity for heat-induced spalling of concrete (e.g. [13, 17, 25]). Polypropylene fibres are theorised to alter the transient moisture migration and/or evaporation processes within heated concrete, thus reducing the propensity for spalling (particularly when a thermo-hydraulic spalling mechanism is dominant). While the mechanisms behind PP fibres' effectiveness remain poorly understood, three potential mechanisms are widely quoted involving the PP fibres generating: (1) discontinuous reservoirs, (2) continuous channels, and/or (3) vacated channels [26].

During heating, rapid volumetric changes of the PP fibres may cause micro-cracks within the concrete matrix surrounding the fibres, thus creating *discontinuous reservoirs* that enhance moisture migration within concrete. Polypropylene fibre inclusion may also promote the formation of discrete reservoirs by inherently increasing air entrainment within the concrete matrix during mixing and casting.

Continuous channels may also be formed at the interfaces between the PP fibres and the concrete matrix due to poor interfacial adhesion and/or a relatively more porous transition zone at the interface. This phenomenon, called *Pressure-Induced Tangential Space (PITS)* theory [26], is postulated as enhancing concrete moisture migration during heating.

Enhanced moisture transport may also be driven by the formation of *vacated channels* left behind by pyrolized (or melted) PP fibres during heating. This is the most widely quoted mechanism used to describe the effect of PP fibres in heated concrete [26], however there is little direct experimental evidence for it [7].

Polypropylene fibres used in concrete applications are commercially available in a range of types and sizes. The most common are monofilament, multifilament, and fibrillated (see Figure 2). Monofilament and multifilament fibres are both manufactured through an extrusion process, with nominal diameters in the range of 10-40 microns. Monofilament fibres are manufactured from a single strand of fibre, while multifilament fibres are made from multiple, combined strands. While the diameter of fibrillated fibres is in the range of monofilament and multifilament fibres, these are manufactured in the form of films that are slit in such a way that they can be expanded into an open network [27] (see Figure 2). Fibres of all types can be cut to the desired length, commonly in the range of 3 to 20 mm. More recently, the use of fibres made out of alternative materials (e.g. polyvinyl alcohol, cellulose, nylon, jute) has been considered, although their effectiveness has yet to be convincingly demonstrated [28].

Despite decades of research, the relative importance of the mechanisms that explain the effectiveness of PP fibre inclusion in reducing the propensity for heat-induced concrete spalling remains a matter of considerable debate [26]. Regardless of the currently unquantifiable propensity for spalling, current design and construction guidance for spalling prevention (e.g. [29, 30]) is solely based on prescribing a dose of polypropylene (PP) fibres which is presumed to assure limited spalling in applications with ‘relatively high’ spalling risk (e.g. high-strength concrete, high in-service moisture content, high in-service compressive stress, rapidly growing fires, etc).

For example, European guidance for concrete in fire [29] recommends including at least 2 kg of monofilament PP fibres per cubic metre concrete for high-strength (>55 MPa cube compressive strength), high moisture content (>3% by mass) and/or concrete with high inclusion of silica fume (>6% by mass of cement). Australian design guidance for concrete in

fire [30] states that the addition of 1.2 kg of 6 mm long monofilament PP fibres per cubic metre concrete has a "dramatic effect in reducing the level of spalling". These (and other) guidelines are based on available experimental research on heat-induced concrete spalling, and can only be viewed as potential means of reducing, rather than eliminating, the occurrence of spalling. Physical mechanisms aside, it is reasonable to assume that an optimum (or most 'effective') PP fibre type and dose ought to exist to mitigate spalling under a given set of conditions [24, 31], without unduly sacrificing other properties such as workability or strength.

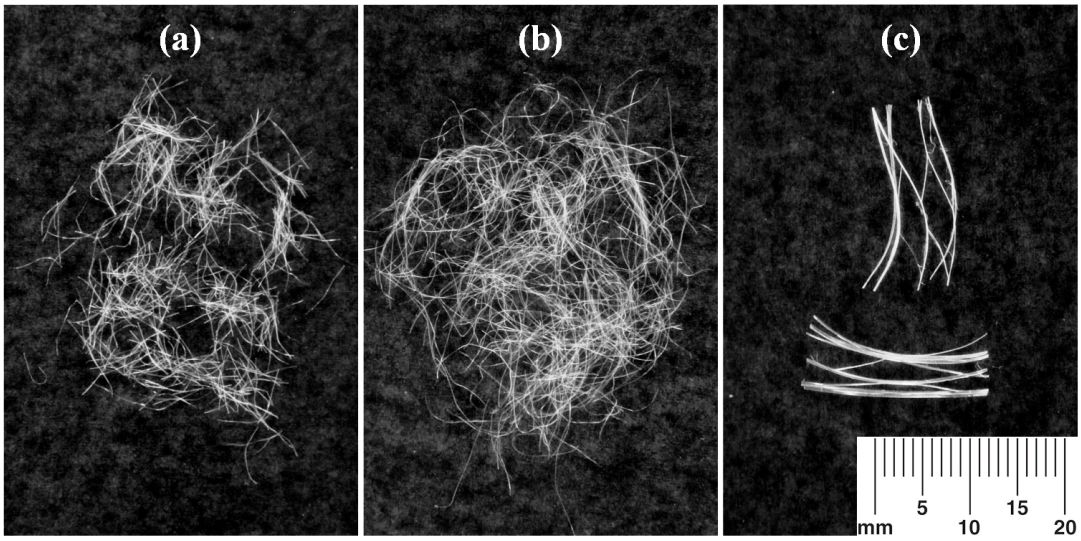

Figure 2 – Photographs of (a) 6 mm monofilament (32 µm diameter), (b) 12 mm multifilament (32 µm diameter), and (c) 20 mm fibrillated (37×200 µm^2) PP fibres.

Within the project presented herein, the occurrence of heat-induced spalling was examined for 11 specific high-performance, self-consolidating concrete (HPSCC) mixes in which PP fibre type, cross-section, length, supplier, and dose were systematically varied (refer to Table 1). Constrained by the manufacturing process needs of an industry project partner (an innovative Swiss precast company), the concrete compressive strength and the workability of the fresh concrete (i.e. slump flow) were maintained constant for all mixes.

The effect of pre-compressive stresses acting on the concrete during testing was also examined, since the end use application of the specific HPSCC mixes studied within the scope of this work involves highly optimized prestressed concrete systems [32]; and since spalling is known to be influenced by in-service stress levels and the development of in-depth differential thermal stresses during heating [7]. The aforesaid highly optimized concrete structural systems have traditionally shown to be extremely vulnerable to the occurrence of spalling [32]. Importantly, rather than seeking to unravel and understand the precise thermo-physical mechanisms contributing to spalling, the current study instead aimed to evaluate the propensity for spalling of the concrete mixes tested under highly repeatable thermal and mechanical conditions; simulating the thermal and mechanical conditions experienced by HPC specimens during a standard fire resistance test (or furnace test).

2 RESEARCH SIGNIFICANCE

Modern HPC mixes demonstrate an increased propensity for heat-induced concrete spalling [7, 8]. Because credibly modelling the occurrence of spalling is not possible at present, due to the complexity of the various mechanisms possibly contributing to spalling, and because of uncertainty around the potential mechanisms behind PP fibres' effectiveness, this paper presents a carefully controlled experimental study on the effectiveness of PP type and dose, using a novel test method to ensure repeatable testing. Moreover, given the considerable expense of performing traditional large-scale fire resistance tests to examine the spalling behaviour of concrete test specimens, the novel test method, a Heat-Transfer Rate Inducing System (H-TRIS), was developed and is used for studying the 'spalling behaviour' of concrete specimens during heating. The novel method permits multiple repeat testing of identical specimens, with outstanding repeatability and at low economic and temporal costs, which has not previously been possible [7].

3 HEAT-TRANSFER RATE INDUCING SYSTEM (H-TRIS)

The novel H-TRIS fire test method was used for studying the propensity for heat-induced spalling of concrete. Rather than taking the traditional approach of controlling the gas temperature inside a fire testing furnace, the H-TRIS test method permits direct and independent control of the thermal boundary condition; it does this by controlling the time-history of incident radiant heat flux, $\dot{q}''_{inc}$, at the exposed surface of a test specimen [33]. H-TRIS (v1.0 of this apparatus was used in the current study) uses a mobile array of propane-fired radiant panels, along with a mechanical linear motion system and a rotary stepper motor (see Figure 3). The linear motion system can be programed to actively control the relative position between the radiant panels and the exposed surface of a test specimen, thus varying incident radiant heat flux at the exposed surface of the test specimen.

For the current study, the imposed thermal boundary condition aimed to replicate the in-depth heating conditions experienced by concrete specimens that had previously been measured during large-scale fire resistance tests of similar specimens and concrete mixes [32]. The specified time-history of imposed incident radiant heat flux aimed to give equivalent in-depth temperature distributions within the concrete as measured during the fire resistance tests. In-depth temperature distributions recorded in large-scale specimens during a set of standard fire resistance tests [32], at 10, 20 and 45 mm from the exposed surface (refer to Figure 4), were used as inputs for an inverse heat conduction model described below.

The time-history of net heat flux, $\dot{q}''_{net}$, needed to simulate the fire resistance tests was determined using an inverse heat conduction model previously developed by the authors [7, 33]. A full description of the inverse model is presented elsewhere, however it is noteworthy that, unlike a traditional heat conduction model in which the thermal boundary condition is assumed and used as an input to calculate the in-depth time-dependent temperature

distributions within a solid, the inverse heat conduction model uses measured in-depth time dependent temperature distributions as inputs to calculate the thermal boundary conditions.

The incident radiant heat flux to be imposed with H-TRIS to give a net heat flux equivalent to that experienced during a fire resistance test was calculated considering the heat flux losses, $\dot{q}''_{losses}$, also accounting for the absorptivity, α_s, at the test specimen's exposed surface (refer to Figure 5), as follows:

$$\dot{q}''_{inc} = \frac{1}{\alpha_s}\left(\dot{q}''_{net} + \dot{q}''_{losses}\right) \quad (1)$$

H-TRIS ensures sufficient spatial separation between the radiant panels and the exposed surface of the test specimen to avoid imposition of vitiated air near the surface of a burning specimen, thus supporting the assumptions used in the inverse modelling procedures and that gases at the exposed surface of the test specimen are not unduly influenced by forced convection from the radiant panels [34].

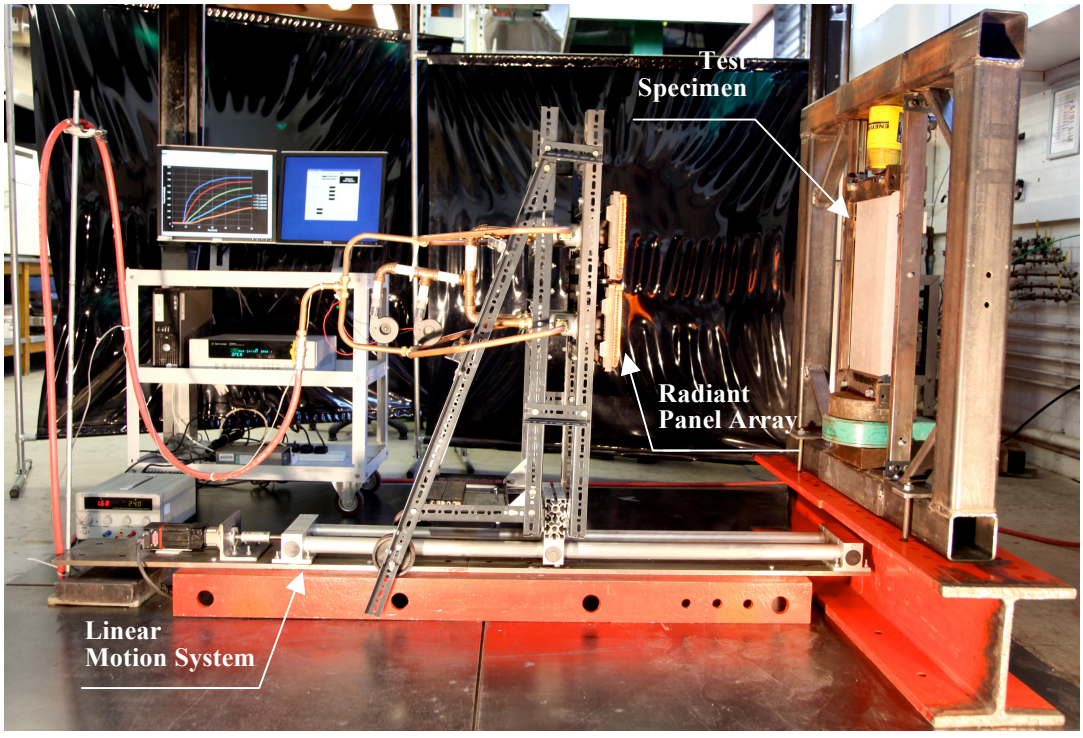

Figure 3 – Photograph of H-TRIS v1.0 (side elevation) [33].

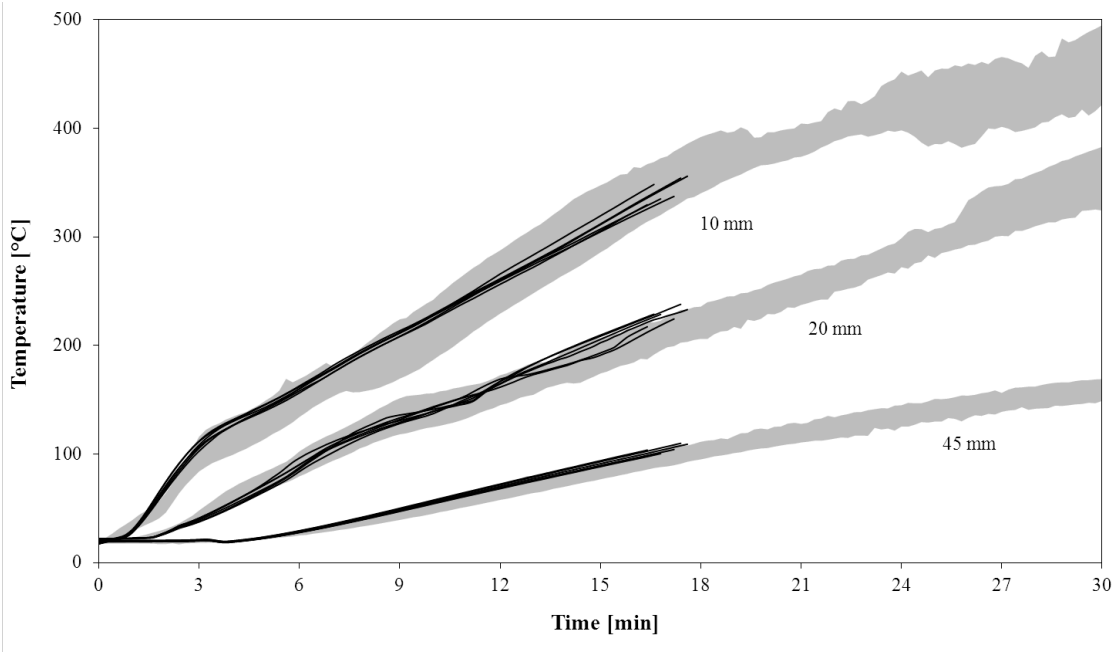

195

196 **Figure 4 – In-depth temperature measurements taken during a standard fire resistance test [32]**
197 **compared against those made with H-TRIS (shaded areas show the spread of temperatures measured**
198 **during a single fire resistance test, black lines show measurements with H-TRIS).**

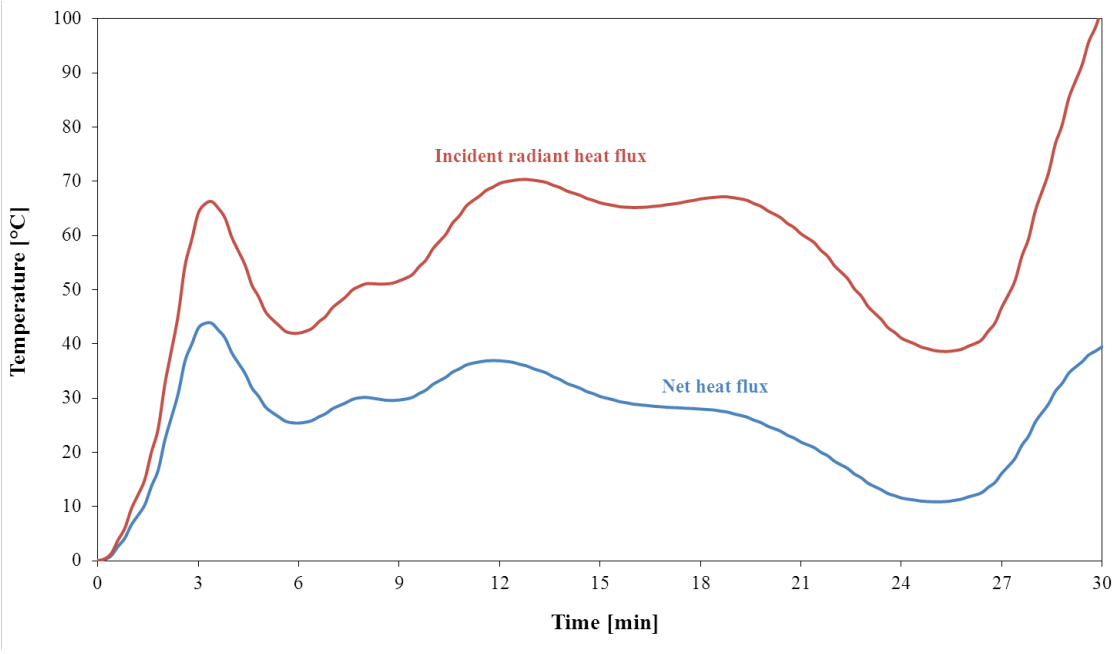

199

200 **Figure 5 – Time-history of net heat flux experienced by test specimens during a standard fire resistance**
201 **test, and calibrated required incident radiant heat flux imposed within H-TRIS to yield an equivalent net**
202 **heat flux at the exposed surface of the test specimen (from inverse modelling).**

203

4 EXPERIMENTAL PROGRAM

Constrained by practical requirements on minimum compressive strength and self-compaction of the concrete mixes; the concrete compressive strength (C90 according to [35]) and workability (slump flow of 750 mm according to [36]) were maintained constant for all concrete mixes studied. Parameters varied amongst the 11 concrete mixes were:

- PP fibre cross-section (18 or 32 μm diameter circular cross-sections, and 37 × 200 μm^2 rectangular cross-sections);
- PP fibre length (3, 6, 12, or 20 mm);
- PP fibre supplier (three manufacturers);
- PP fibre type (monofilament, multifilament, or fibrillated); and
- dose (between 0.68 and 2.34 kg of PP fibres per m^3 of concrete).

Mix labels shown in Table 1 and Table 2 have no inherent meaning but were defined by the industrial partner based on an in-house mix numbering scheme. Specific PP fibre suppliers are named purely for the purposes of factual accuracy. The fibre doses given in Table 1 were chosen to provide, to the extent possible, like-for-like comparisons assessing: (1) the fibre dose (i.e. total fibre mass), (2) the total fibre surface area, (3) the total fibre length, (4) the total number of individual fibres per unit volume of concrete; all while maintaining consistent compressive strength and self-consolidating properties.

223 **Table 1 – Description of PP fibres included in the concrete mixes evaluated.**

Mix Label	PP Fibre Parameters			Like-for-like Comparison			
	Supplier (type)	Cross-section	Length	Dose [kg/m^3]	Total fibre surface area [m^2/m^3]	Total fibre length [km/m^3]	Total number of individual fibres [mill. of fibres/m^3]
042*	None				-	-	-
132	Bekaert[a] (monofilament)	18 µm	6 mm	0.68	165	2915	486
142		32 µm		1.20	165	1640	273
341*	Propex[b] (multifilament)	32 µm	3 mm	1.20	165	1640	547
342				2.00	275	2733	911
345			6 mm	1.20	165	1640	273
343				1.40	192	1913	319
344			12 mm	1.20	165	1640	137
241*	Vulkan[c] (fibrillated)	37×200 µm^2	20 mm	1.20	84	178	15
242*				2.00	141	297	25
243				2.34	165	348	29

*Concrete mixes for which spalling occurred during testing.

[a] www.bosfa.com/products/duo-mix-fire.aspx

[b] www.fibermesh.com/product/microsynthetic.html

[c] www.en.krampeharex.com/pdf/Kunststofffaser_PF.pdf

224

225 **Table 2 – Description of the constituents and properties of the concrete mixes evaluated.**

Mix Label	Water/Cement [1]	Limestone aggregate (0-8 mm)	Super-plasticizer	Slump flow [36]	Moisture content at testing	Compressive strength (Standard deviation)	
						28 days	6 months
	[-]	[kg/m^3]	[% of cement]	[mm]	[%]	[MPa]	[MPa]
042*	0.33	1745	1.73 %	808	4.5 %	101 (1.6)	106 (1.3)
132	0.32	1710	1.70 %	740	4.4 %	95 (1.1)	105 (0.7)
142	0.31	1708	1.71 %	745	4.3 %	95 (2.7)	109 (0.3)
341*	0.32	1716	1.67 %	800	4.0 %	103 (0.8)	112 (0.6)
342	0.33	1726	1.73 %	765	4.6 %	98 (2.1)	107 (1.1)
345	0.31	1715	1.72 %	758	4.5 %	104 (0.6)	108 (0.6)
343	0.32	1711	1.71 %	740	4.3 %	99 (1.0)	105 (0.9)
344	0.31	1711	1.73 %	740	4.5 %	101 (0.4)	108 (0.7)
241*	0.31	1724	1.65 %	765	4.0 %	103 (0.6)	106 (0.6)
242*	0.35	1729	1.73 %	740	5.0 %	94 (1.1)	108 (0.5)
243	0.33	1685	1.68 %	680	4.6 %	95 (1.4)	103 (0.4)

[1] **Cement constituents:** 64% Portland cement, 16% microsilica, 20% fly ash.

*Concrete mixes for which spalling occurred during testing.

4.1 Test specimens

Medium-scale unreinforced and unstressed concrete specimens were tested using H-TRIS in a vertical orientation with heating from one side. Recognising that scaling of test specimens in structural fire resistance testing is debated on various grounds [7], the dimensions of the specimens in the direction of the principal heat flow were taken as the same as those used for the prior large-scale furnace test specimens [32]. Thus, medium-scale specimens had 45 × 200 mm^2 cross-sections and an overall length of 500 mm (due to space limitations within H-TRIS). Cold overhangs (i.e. unheated ends) with a length of 50 mm were required due to specimen holding and loading considerations; thus the thermally exposed surface was 400 × 200 mm^2, as shown in Figure 6.

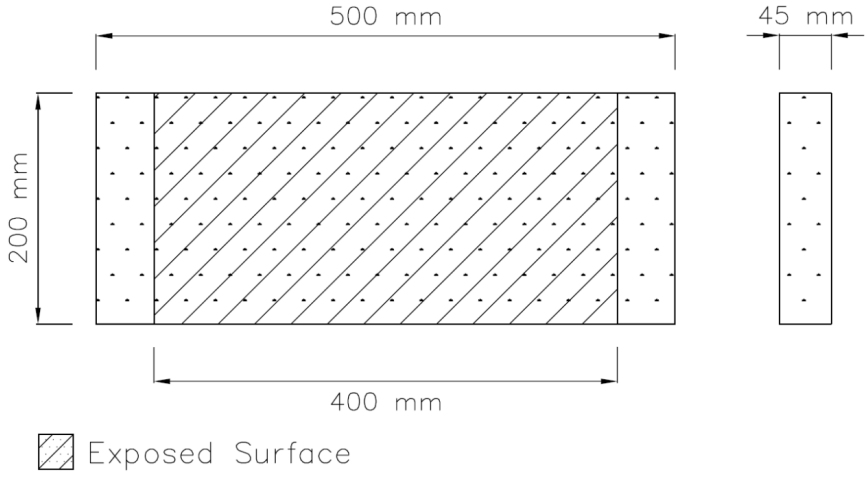

Figure 6 – Plan and section views of concrete specimens tested with H-TRIS.

4.1.1 Casting and curing process

Specimens were cast in the production facilities of the industry partner. The mixing and casting procedures were performed according the standards for typical precast concrete elements fabricated by the industry partner. While the parameters of the concrete mixes were predefined, as shown in Table 2, maintaining certain key parameters unchanged, mild

variations during the concrete mixing process were required to attain the optimum self-compacting characteristics required for constructability (i.e. a minimum slump flow of about 750 mm). This was mainly attributed to the variable (and uncontrolled) conditions during casting (e.g. moisture content of the aggregates used, ambient temperature, ambient humidity, etc.); however these changes are not considered relevant for the current study. Constituents and slump flow values [36] for the various concrete mixes are given in Table 2.

After casting in Switzerland, specimens were covered with polyethylene sheeting for 48 hours before stripping the forms, and were cured in moist conditions under polyethylene sheets for a further 3 to 5 months before being delivered to the UK for testing. They were then stored in a conditioning room at 20°C and 80% relative humidity (RH) until testing. All specimens were tested at an age between 13 and 16 months from casting.

Cubes (150 mm) were cast for compressive strength and average moisture content measurements and kept under identical curing conditions. The average moisture content of the test specimens at the time of testing was between 4.0 and 5.0% by mass; these measurements being made by dehydration mass loss. Compressive strengths at 28 days and 6 months were between 93 and 112 MPa [35]. Table 2 presents the moisture and compressive strength measurements for each of the specific mixes.

4.2 Test procedure

As previously explained, H-TRIS was programmed to impose a thermal boundary condition equivalent to that experienced by the large-scale concrete specimens tested during standard fire resistance tests [32]. Figure 5 shows the time-history of incident radiant heat flux yielding an equivalent time-history of net heat flux, and hence equivalent in-depth temperature distributions as experienced during the fire resistance tests.

The maximum possible incident radiant heat flux that could be achieved in H-TRIS v1.0 is 100 kW/m^2. The desired time-history of incident radiant heat flux shown in Figure 5 was therefore imposed until the maximum incident radiant heat flux of 100 kW/m^2 was reached; beyond this point it was maintained constant at 100 kW/m^2. Because the objective of the study was to examine the spalling behaviour (or more specifically, the occurrence of the first spalling event), rather than to develop a deep understanding of the specific mechanisms involved, tests with H-TRIS were continued only until first spalling event occurred; if no spalling occurred within 60 minutes the test was halted, since heat-induced explosive spalling is unlikely at late stages [7].

It was desired to also examine the effect of pre-compressive stresses on propensity for spalling during testing. Mechanical loading and boundary conditions were imposed using a purpose built loading rig (see figures 3 and 7), designed to impose a sustained axial compressive loading on the test specimens during heating, hence replicating the pre-compression that would be experienced by prestressed concrete specimens manufactured from similar concrete mixes (recall that the specimens tested with H-TRIS were unreinforced and un-prestressed, however the end use applications envisioned for these mixes are typically precast, prestressed). For reasons described elsewhere [32], the loading in H-TRIS aimed to replicate the conditions near the ends of the prestress transfer zones of prestressed HPC specimens with nominally concentric prestressing forces (i.e. with prestressing at mid-depth).

Specimens were tested either under a free-to-expand (unrestrained) condition or under sustained compressive load. Based on prior research [7], the service pre-compressive stress within the concrete at the end of a prestress transfer zone was conservatively defined as 12.3 MPa (i.e. prestressing losses due to elastic shortening, shrinkage, creep effects, and thermally induced prestressing forces were neglected). Therefore, the sustained axial compressive load

applied on specimens tested in H-TRIS, which has cross-sectional areas of 9000 mm^2 (200 × 45 mm), was:

$$L_{c,0} = 12.3[\text{MPa}] \cdot 9000[\text{mm}^2] = 110.7[\text{kN}] \quad (1)$$

This concentric compressive load, $L_{c,0}$, was applied using notionally rotationally fixed-fixed end conditions. Load was held constant for the duration of the tests using a hydraulic load control system (i.e. the applied compressive load was maintained, counteracting potential effects from thermal expansion and elastic modulus changes of the test specimen during heating). Unloaded test specimens were left free-to-expand (under notionally rotationally fixed-fixed end conditions) during heating. All tests were performed in triplicate for each specific concrete mix and restraint condition.

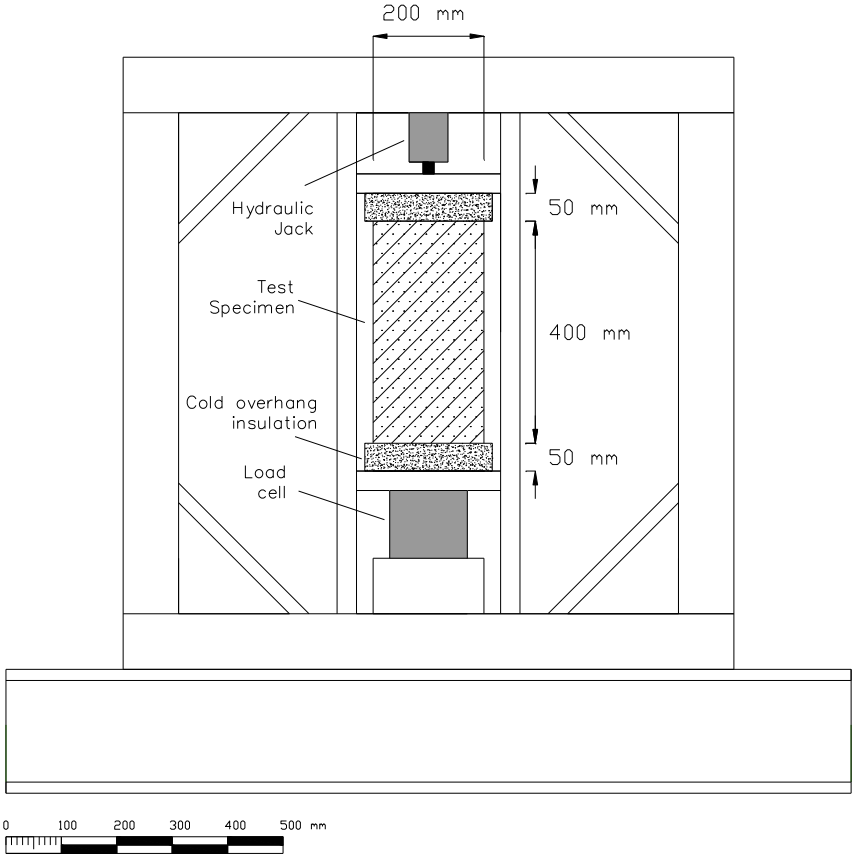

Figure 7 – Schematic showing the mechanical loading rig used in H-TRIS testing (front elevation).

4.3 Assessment of spalling

With a few exceptions (e.g. [37]), the propensity and extent of concrete spalling during fire tests is traditionally assessed only by visual evaluation of the specimens' exposed surface, and occasionally by measuring the depth, volume, or mass of spalled concrete. Testing with H-TRIS allows a more careful quantification of time-to-spalling, the mass of concrete spalled, and the total net heat density up to the moment of first spalling; this is calculated as the area under the time versus net heat flux curve divided by the area of the exposed surface.

5 TEST RESULTS AND ANALYSIS

Sixty-six individual spalling tests were performed during a period of 30 days; thus demonstrating the low temporal costs of the H-TRIS testing approach as compared with traditional furnace testing; this number of tests would have taken months using a standard fire testing furnace.

It is noteworthy that (contrary to expectations and contrary to most prior research on spalling performed in furnaces), when spalling occurred for a given mix tested in H-TRIS it occurred for all three identical repeat tests, and at similar heating exposure times. Likewise, if no spalling was observed for a particular mix with H-TRIS then this was true for all three repeat tests. Figure 8 shows typical post-test photographs of H-TRIS test specimens showing increasing severities of spalling.

Spalling occurred for four of the 11 concrete mixes, namely: 042, 341, 241, and 242 (refer to tables 1 and 2). None of the other mixes experienced any spalling whatsoever for the full duration of the 60 minute tests. A summary of the relevant test results for the concrete mixes that experienced spalling is given in Table 3 (non-spalling mixes are not included).

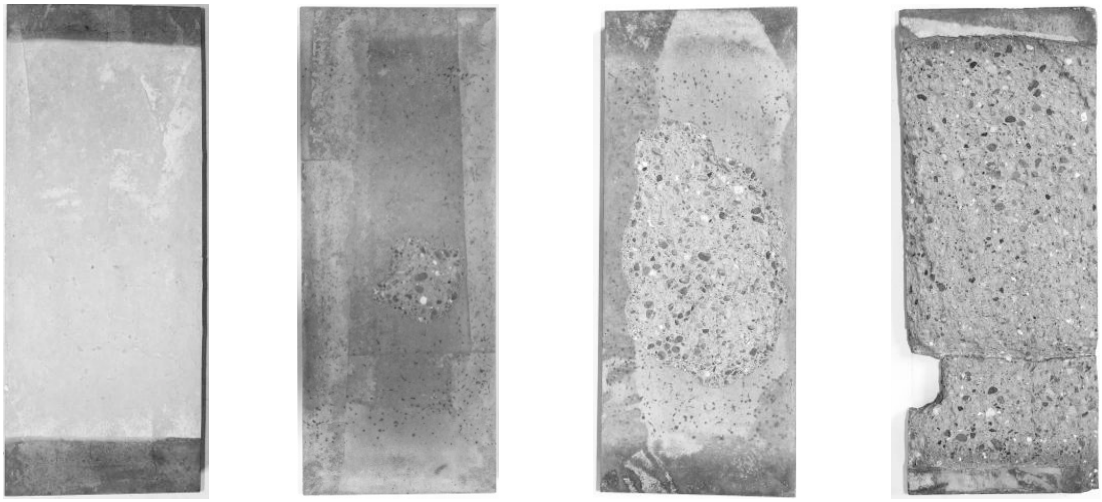

Mix 342	Mix 241	Mix 242	Mix 341
(no spalling)	(100 g spalled)	(1503 g spalled)	(3095 g spalled)

Figure 8 – Post-test photographs of specimens tested with H-TRIS [38].

328 **Table 3 – Experimental test matrix and results for spalled specimens tested with H-TRIS.**

Mix	Sustained compressive stress	Time to spalling	Net Heat Density	Mass spalled [1]		Mass spalled /net heat density
		[min]	[kJ/cm^2]	[g]	[%]	[g × cm^2 / kJ]
042	0 MPa	10.9	2.28	208	2.0 %	91
		24.7	5.99	664	6.3 %	111
		13.9	3.01	1135	10.7 %	377
	12.3 MPa	12.5	2.66	1281	12.1 %	481
		11.0	2.31	679	6.3 %	294
		13.1	2.81	1189	11.2 %	424
341	0 MPa	17.1	3.85	923	8.4 %	240
		14.6	3.19	268	2.4 %	84
		16.5	3.67	435	4.0 %	118
	12.3 MPa	16.3	3.64	3095	28.5 %	850
		13.0	2.80	2043	18.7 %	731
		14.4	3.16	2645	24.4 %	838
241	0 MPa	12.4	2.66	420	3.8 %	158
		7.9	1.61	100	0.9 %	62
		11.7	2.49	238	2.2 %	96
	12.3 MPa	7.3	1.48	251	2.3 %	169
		14.3	3.11	210	1.9 %	67
		12.5	2.66	784	7.2 %	294
242	0 MPa	-	-	-	-	-
		-	-	-	-	-
		-	-	-	-	-
	12.3 MPa	9.9 [2]	2.07	438	4.1 %	212
		9.4 [2]	1.93	423	4.0 %	219
		10.6 [2]	2.22	1503	14.3 %	678

[1] Mass spalled was calculated by subtracting the mass of the tested specimen (after cooling) from the initial mass of the specimen. Note that no distinction is made between mass lost due to the spalled concrete and that due to dehydration of the specimen during heating.

[2] Large-scale prestressed specimens tested during standard fire resistance tests [32] spalled during the first 9.2 to 10.3 minutes from the start of the test.

5.1 Assessment of spalling

When testing using H-TRIS it is possible to accurately quantify the time-to-spalling, the mass spalled, and the accumulated net heat density. All three quantifiable metrics are described below.

5.1.1 Time-to-spalling

During the tests described herein, when heat-induced spalling of concrete occurred it was always between 7 and 25 minutes from the start of the test (refer to Table 3). This being said, time-to-spalling demonstrated no obvious correlations with other parameters investigated herein.

The occurrence of heat-induced concrete spalling was in reasonable agreement in terms of time-to-spalling (i.e. ±2 minutes) with specimens cast from identical concrete mixes and tested during the aforementioned large-scale fire resistance tests [32] (refer to Table 3). This observation provides further credence to H-TRIS' ability to accurately replicate not only the in-depth time dependent temperature distributions experienced by concrete specimens during standard fire resistance tests, but also the time-to-spalling during repeat testing of identical specimens under identical thermal boundary and loading/restraint conditions.

5.1.2 Mass spalled

Specimens' masses were measured before and after each test. For tests where spalling occurred the mass lost as a consequence of the spalling event and *dehydration* was calculated by subtracting the mass of the tested specimen (after cooling) from the initial mass of the specimen. It is noteworthy that no distinction was made between mass lost due to the spalled concrete and the mass lost due to dehydration of the specimen during heating.

Figure 9 shows the percentage of mass spalled plotted against the time-to-spalling for tests under a free-to-expand condition and under sustained compressive stress. Whilst the trend is not categorical, in most cases the test results indicate that when spalling occurs at an early stage of the test the mass spalled is lower than when it occurs at a later stage. For example, an exception to the aforesaid trend was observed for one of the test specimens cast with Mix 042 (no PP fibres), which spalled after 25 minutes from the start of the test and showed a relatively low percentage of mass spalled (refer to Table 3 and Figure 9). This may be associated with the fact that longer heating periods result in higher amounts of accumulated thermal (and thermo-mechanical) energy, which predictably results in more energy being released upon spalling; thus more concrete mass spalled.

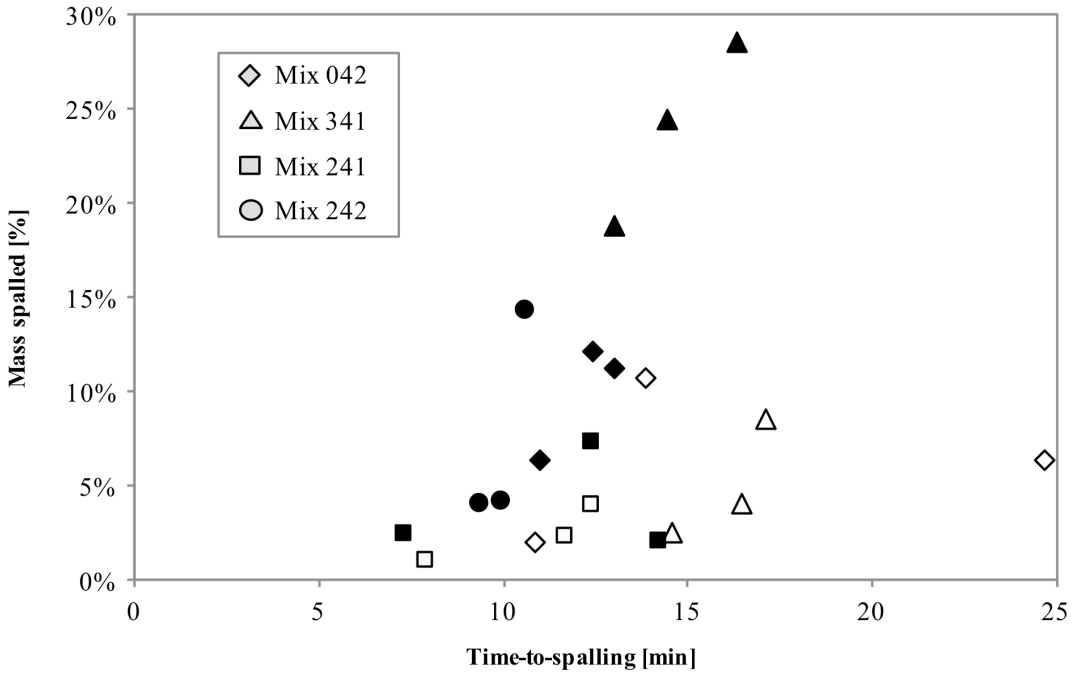

Figure 9 – Percentage of mass spalled versus time-to-spalling for tests in free-to-expand condition (filled markers) and tests under sustained compressive stress (empty markers).

5.1.3 Accumulated net heat density

The ratio of mass spalled to accumulated net heat density was calculated for each of the spalled test specimens (refer to Table 3). This ratio could potentially allow for rational,

quantifiable comparison between spalling events for concrete specimens tested under different thermal boundary conditions. Although this variable heat flux comparison was not carried out in the current study, the concept is first introduced here and will be used in future studies in which the effect of different thermal boundary conditions is evaluated using H-TRIS.

5.2 Parametric analysis

This section presents a parametric assessment performed for each of the PP fibre parameters varied within the current study, with reference to Table 1.

5.2.1 PP fibre cross-section

As is widely recognized by concrete manufacturers and researchers (e.g. [24, 31]), during the casting process it was observed that PP fibres with a small cross-sections (i.e. 18 μm diameter) had a strong undesirable effect on the self-compacting and workability of the fresh concrete mixes, thus the required slump flow was attained only for a relatively low dose of these smaller cross-section fibres (refer to Table 1). For instance, similar slump flow was achieved for two mixes, 132 and 142, respectively. Mix 132 included 0.68 kg of 18 μm diameter PP fibres per m^3 of concrete and had a slump flow of 740 mm, whereas Mix 142 had a slump flow of 745 mm with a larger dose of 1.20 kg of 32 μm diameter PP fibres per m^3 of concrete (refer to Table 2). Mix 142 thus had almost double the dose (by mass) of PP fibres, while all other parameters (e.g. PP fibre length, supplier, type, etc.) were unchanged (refer to Table 1).

No spalling was observed for mixes 132 or 142 (both mixes including 6 mm long monofilament PP fibres), thus no direct comparisons were possible to evaluate the influence of cross-section on spalling for identical monofilament PP fibres with circular cross-sections

390 of 18 or 32 μm in diameter. Nonetheless, it appeared that including 0.68 kg per m^3 of 18 μm
391 diameter PP fibres was 'as effective' as including 1.20 kg per m^3 of 32 μm diameter fibres for
392 the time history of heat flux considered in the current study (simulating the exposure during a
393 standard fire resistance test [32]).

394 Concrete specimens cast with mixes including fibrillated PP fibres with comparatively large
395 37×200 μm^2 rectangular cross-sections (i.e. mixes 241, 242 and 243) demonstrated a high
396 occurrence of spalling, although a 'recommended' [35] dose of PP fibres was included (i.e.
397 2.00 kg of PP fibres per m^3 in Mix 242). Test specimens cast with Mix 241 (1.20 kg of PP
398 fibres per m^3) spalled both when tested under sustained compressive stress and under free-to-
399 expand conditions (refer Table 3). Specimens cast with Mix 242 (2.00 kg of PP fibres per
400 m^3), equivalent to that for casting of large-scale prestressed specimens tested in a standard
401 fire resistance test [32] only spalled when under sustained compressive stress; unstressed
402 specimens did not spall. Specimens cast with Mix 243 (2.34 kg of PP fibres per m^3 of
403 concrete) did not spall under any condition.

404 *5.2.2 PP fibre length*

405 A comparison was made to assess the influence on spalling of individual PP fibre length for
406 concrete mixes 341, 345, and 344, all of which included 1.20 kg of PP fibres per m^3 of
407 concrete (32 μm in diameter multifilament PP fibres) with PP fibre lengths of 3, 6 and 12
408 mm, respectively (refer to Table 1). Spalling was observed for all specimens with 3 mm long
409 PP fibres (refer to Table 3), which suggests a negative influence of using very short PP fibres,
410 thus supporting the theoretical findings from prior studies; relatively short PP fibres fail to
411 generate so-called *continuous channels* (refer to Section 1.2) for enhancing moisture
412 migration during heating thought [4, 31]. For the current study, 3 mm long PP fibres were
413 considered because of their reduced influence on the workability of fresh concrete. Very long

PP fibres have a clear negative impact on the self-compacting and workability properties of fresh concrete; i.e. at an equivalent dose the use of longer PP fibres results in lower measured slump flow (refer to Table 2). No spalling was observed for either of the other two mixes, providing no clear comparative data for 6 mm versus 12 mm long PP fibres.

5.2.3 PP fibre supplier

The PP fibre suppliers whose products were assessed in this study were Bekaert, Propex, and Vulkan. No spalling was observed for mixes 142 and 345 cast with an equivalent dose (1.20 kg of PP fibres per m^3 of concrete) of basically identical PP fibres from different suppliers (32 μm diameter, 6 mm long monofilament and multifilament PP fibres); hence, as expected, no influence was observed for the comparison made between these essentially identical concrete mixes.

5.2.4 PP fibre type

Concrete mixes which included monofilament or multifilament PP fibres showed a lower propensity for heat-induced concrete spalling relative to those cast with fibrillated PP fibres. This may not only be associated to the type of PP fibre but to the significantly larger cross-section of the fibrillated PP fibres (refer to Table 1); hence the inevitably lower specific surface area of individual fibres (discussed in Section 5.3.2).

5.2.5 Sustained compressive stress

For mixes in which spalling occurred under sustained compressive stress, spalling also occurred under free-to-expand conditions; with the exception of Mix 242 (refer to Table 3) which did not spall under a free-to-expand condition but spalled in all cases when under sustained compressive stress. This corroborates that widely stated belief that stressed concrete is more likely to spall than unstressed concrete, all other factors being equal.

5.3 Like-to-like comparisons

In addition to the parametric analysis presented herein, three additional parameters associated with the inclusion of PP fibres were compared on a like-to-like basis (refer to Table 1).

5.3.1 Dose of PP fibres

The concrete mixes examined in the current study had a range of doses between 0.68 and 2.34 kg of PP fibres per m^3 of concrete. An explicit comparison between specific mixes (refer to Table 1) was carried out to assess the influence of PP fibre dose (keeping all other parameters constant) on the occurrence of spalling:

- Mixes 341 (spalled) and 342 (did not spall) included 1.20 and 2.00 kg of PP fibres per m^3, respectively (multifilament fibres 32 μm in diameter and 3 mm long).

- Mixes 345 and 343 (neither of which spalled) included 1.20 and 1.40 kg of PP fibres per m^3, respectively (multifilament fibres 32 μm in diameter and 6 mm long).

- Mixes 241 (spalled), 242 (spalled only when loaded), and 243 (did not spall) included 1.20, 2.00 and 2.34 kg of PP fibres per m^3, respectively (fibrillated fibres with 37×200 μm rectangular cross-section and 20 mm long).

It is noteworthy that spalling occurred for all test specimens cast from Mix 042, which had no PP fibres (refer to Table 1). As expected, a higher dose of PP fibres resulted in a lower propensity for heat-induced concrete spalling. This is clear when comparing the test results for mixes 341 and 342, as well as those for mixes 241, 242, and 243. Obviously, the inclusion of high doses of PP fibres has an undesirable effect on the self-compacting and workability properties of fresh concrete; hence future work with H-TRIS will focus on defining optimum

458 PP fibre doses to meet competing goals of spalling mitigation and practical workability of
459 concrete mixes for use in various types of structural applications.

460 It should be noted that test results for mixes 132 and 142 (6 mm long monofilament PP
461 fibres) suggested that including a dose of 0.68 kg per m^3 of 18 μm diameter PP fibres was as
462 effective as including 1.20 kg per m^3 of 32 μm diameter fibres; similar slump flow was
463 measured for these mixes (refer to Table 1), hence it is not necessarily the dose of PP fibres
464 alone that defines their effectiveness in spalling mitigation.

465 *5.3.2 Total PP fibre surface area*

466 Khoury [26] proposed the hypothesis that the existence of discontinuous reservoirs (at
467 ambient and at high temperatures) is further promoted by the inclusion of PP fibres. This
468 hypothesis suggests that at ambient temperature the presence of PP fibres promotes the
469 creation of discrete reservoirs (i.e. air entrainment) in the concrete pore structure, whereas at
470 elevated temperatures PP fibres create discontinuous reservoirs by micro-cracking the
471 surrounding concrete matrix when undergoing volumetric and phase changes during heating.
472 This potentially explains the positive influence of PP fibres in altering the moisture migration
473 and/or evaporation within heated concrete, thus possibly accounting for their observed effects
474 in reducing the propensity for heat-induced concrete spalling. Based on this hypothesis; the
475 total surface area of PP fibres could potentially be a key parameter to explain the positive
476 influence of PP fibres. Mixes 132, 142, 345, and 344 had equivalent total surface areas of PP
477 fibres; this being 165 m^2 of PP fibre surface area per m^3 of concrete in all cases (refer to
478 Table 1). Although mix 341 had 165 m^2 of PP fibre surface area per m^3 of concrete, a high
479 propensity for spalling was observed due to the negative effect of relatively short (3 mm) of
480 the PP fibres included in this mix (as noted in the parametric analysis above).

5.3.3 Total PP fibre length

Khoury [26] also hypothesized that changes in the pore structure of concrete, and therefore reductions in the propensity for heat-induced concrete spalling, are driven by the creation of continuous channels in the cement matrix. Based on this hypothesis, the total length of PP fibres could also potentially be a key parameter to explain the positive influence of PP fibres in mitigating the propensity for spalling. Mixes 142, 345, and 344 had an equivalent total length of PP fibres; this being 1640 km of PP fibres per m^3 of concrete (refer to Table 1). Yet again, while mix 341 had 1640 km of PP fibres per m^3 of concrete, a high propensity for spalling was observed due to the negative effect of the relatively short (3 mm) PP fibres included in this mix. Thus total PP fibre length also appears not to be a fundamental parameter.

5.3.4 Total number of individual PP fibres

It is widely stated in the literature that a higher number of individual PP fibres (as well as a higher dose of PP fibres) enhances the effectiveness in reducing the propensity for heat-induced concrete spalling [31]. Nonetheless, spalling occurred for all specimens cast with Mix 341 (32 μm diameter, 3 mm long multifilament PP fibres with) which had a relatively high number of individual PP fibres (547 million individual PP fibres per m^3 of concrete). This suggests the relevant influence of individual fibre length on the effectiveness of PP fibres in reducing the propensity for heat-induced concrete spalling that warrants further investigation.

To summarise, mixes with an equal or higher value of total surface area or total length of PP fibres to those of the predefined values compared in this study (165 m^2 or 1640 km of PP fibres per m^3 of concrete) did not spall (refer to Table 1). Furthermore, test specimens cast with mixes 241 and 242, both of which had significantly lower values of all of the like-to-like

parameters examined in the current section, spalled during testing. No spalling was observed for Mix 243, although it also had low values of total length of PP fibres and total numbers of PP fibres, however with a high total surface area of PP fibres (165 m^2 of PP fibres per m^3 of concrete). This suggests a possible relevance of total surface area of PP fibres as compared to the total length or number of individual PP fibres.

5.4 Experimental validation of the thermal exposure

Three additional medium-scale concrete specimens were cast with concrete Mix 042 (refer to tables 1 and 2) and instrumented with in-depth thermocouples (K-type) placed at equivalent depths to those placed in the aforementioned large-scale furnace test specimens which have been described elsewhere [32]; namely at 10, 20 and 45 mm from the exposed concrete surface. These specimens were tested with H-TRIS, and in-depth temperature distribution measurements were used to verify that the thermal boundary conditions imposed with H-TRIS were indeed equivalent to those experienced by otherwise identical specimens during standard fire resistance tests.

Figure 4 gives a comparison of in-depth temperature measurements between effectively identical concrete elements (identical in the direction of the principal heat flow) during fire resistance tests (shaded areas) and tested with H-TRIS (black lines), and shows very good agreement. This comparison verifies the use of H-TRIS, particularly for replicating the in-depth temperature distribution experienced by concrete specimens during the fire resistance tests performed by Terrasi et al. [32]. Figure 4 also illustrates the excellent repeatability of testing with H-TRIS (three repeat tests are shown with two temperature measurements at each depth) as compared with the greater variability observed in fire resistance tests described in this paper (three repeat tests are shown with one temperature measurement at each depth).

6 CONCLUSIONS

The studies described herein represent the first experiments ever performed using the novel H-TRIS testing methodology and apparatus to simulate the net heat flux at the exposed surface, and hence the in-depth time dependent temperature distributions within concrete specimens, during an otherwise identical standard fire resistance test. The study aimed at examining the propensity for heat-induced concrete spalling of 11 HPSCC mixes in which the PP fibre type, cross-section, length, supplier, and dose were systematically varied.

The inclusion of PP fibres has a clear positive effect on reducing the propensity for heat-induced concrete spalling. Additionally, based on the parametric analysis and discussion presented herein, the following overall conclusions can be made on the various factors that may have an impact on PP fibre effectiveness at spalling mitigation of the HPSCC mixes examined within the scope of this study:

- *PP fibre cross-section* – inclusion of PP fibres with smaller cross-sections has a positive influence in reducing the propensity for spalling.

- *PP fibre length* – mixes cast with relatively short (3 mm long) PP fibres exhibit a higher propensity for spalling than practically identical mixes (equivalent PP fibre dose) with longer fibres (6 or 12 mm long); thus, longer PP fibres appear to be more effective at reducing the propensity for spalling.

- *PP fibre supplier* – the comparison made between PP fibres manufactured by Bekaert, Propex, and Vulkan showed that fibre supplier has no obvious influence on spalling (all other factors being equal).

- *PP fibre type* – monofilament or multifilament PP fibres type showed a lower propensity for heat-induced concrete spalling relative to those cast with fibrillated PP fibres. This

552 may be associated with the lower specific surface area of larger cross-section fibrillated
553 PP fibres.

554 • *Sustained compressive stress* – specimens for which spalling occurred under sustained
555 compressive stress also suffered from spalling when tested under a free-to-expand
556 conditions (with exception of Mix 242, which confirmed an influence of pre-compressive
557 stress for this particular mix).

558 Based on the like-to-like comparisons presented, the following conclusions can be made:

559 • *Dose of PP fibres* – as expected, high doses of PP fibres have a positive influence in
560 mitigating the occurrence of spalling; however some very low doses, e.g. Mix 132 (0.68
561 kg of PP fibres per m^3 of concrete), of specific PP fibres (e.g. those of relatively small
562 cross-section) were also effective at reducing the propensity for spalling, and some
563 comparatively high doses , e.g. Mix 242 (2.00 kg of PP fibres per m^3 of concrete), were
564 not. This suggests that current guidance for mitigation of spalling in HPC [29] is hard to
565 defend scientifically and requires revision.

566 • *Total PP fibre surface area, total PP fibre length, and total number of individual PP*
567 *fibres* – results showed that concrete mixes with relatively high values of total PP fibres
568 surface area, total PP fibre length, and total number of individual PP fibres were effective
569 in reducing the propensity for heat-induced concrete spalling. However, the mix that
570 included 3 mm long monofilament PP fibres had high values of all of these parameters;
571 yet displayed a high propensity for spalling. Moreover, no spalling was observed for Mix
572 243 which included 20 mm long fibrillated PP fibres at a comparatively high dose of
573 2.34 kg of PP fibres per m^3 of concrete. Although this mix had low values of total PP
574 fibre length and the total number of PP fibres, it had a similar total surface area of PP

fibres to other mixes (165 m^2 of PP fibres per m^3 of concrete). This suggests a relevance of the total surface area of PP fibres over the total PP fibre length or total number of PP fibres, while assuming that the shape of the cross section (rectangular or circular) is negligible.

The inclusion of PP fibres has an obvious negative effect on slump flow values. Polypropylene fibres with reduced cross-section and/or large individual lengths showed a more negative influence on slump flow, compared to PP fibres with increase cross-section and short individual lengths. Inclusion of PP fibres showed no obvious influence on moisture content or compressive strength.

Based on the use of H-TRIS within the scope of the work carried for the study described herein, the following observations may be made in regards to the novel test method:

- Test results verified the use of H-TRIS, particularly for simulating specified in-depth temperature distributions and time-to-spalling experienced by concrete specimens during the large-scale furnace test presented by Terrasi et al. [32]; providing excellent repeatability at a low economic and temporal cost and with outstanding repeatability.

- The use of H-TRIS allowed accurate quantification of the time to first spalling, the mass spalled, and the net heat density of the tested specimens. Spalling occurred between 7 and 25 minutes from the start of the test. When spalling occurred, the mass spalled from tested specimens was between 0.9 and 28.5% of the total weight of the specimen before testing; in most cases the test results indicate that when spalling occurs at an early stage of the test the mass spalled is lower than when it occurs at a later stage.

ACKNOWLEDGEMENTS

The authors would like to thank SACAC Schleuderbetonwerk AG and The University *of* Edinburgh, and in particular Lukas Bäurle, Nunzio Spano, Birol Kanik, and Etienne Dessendier. This research was partially funded by the BRE Centre for Fire Safety Engineering at The University of Edinburgh and Empa. Arup and the Royal Academy of Engineering are gratefully acknowledged for their ongoing support of Arup Prof Bisby.

REFERENCES

[1] Bilow D.N. and Kamara M.E. Fire and Concrete Structures. Proceedings of the *ASCE Structures Congress 2008: Crossing Borders*, Vancouver, Canada, 2008, 10 pp.

[2] Mehta P.K. and Aïtcin P.C. Principles Underlying Production of High-Performance Concrete. *ASTM - Cement, Concrete, and Aggregates*, 1990, 12 (2), 70-78.

[3] Walraven J. High-Strength Concrete in the Netherlands. *American Concrete Institute Special Publication on High Strength Concrete: An International (ACI SP-167-5)*, 1997, 103-126.

[4] Bentz D.P. Fibers, Percolation, and Spalling of High Performance Concrete. *ACI Materials Journal*, 2000, 97 (3), 351-359.

[5] Kodur V.K.R. and Phan L. Critical Factors Governing the Fire Performance of High Strength Concrete Systems. *Fire Safety Journal*, 2007, 42 (6-7), 482-488.

[6] Mehta P.K. Advancements in Concrete Technology. *Concrete International*, 1999, 21 (6), 69-76.

[7] Maluk C. Development and Application of a Novel Test Method for Studying the Fire Behaviour of CFRP Prestressed Concrete Structural Elements. PhD Thesis, *The University of Edinburgh*, UK, 2014, 473 pp.

[8] Boström L. and Jansson R. Fire Resistance. *RILEM TC 205-DSC: State-of-the-Art Report*, 2007, 143-152.

[9] Miller R.P. Legislation Concerning the Use of Cement in New York City. Proceedings of the *National Association of Cement Users*, 1906, 186-197.

[10] Hull W.A. and Ingberg S.H. Fire Resistance of Concrete Columns. *Technologic Papers of The Bureau of Standards (No.272)*, 1925, 635-708.

[11] Meyer-Ottens C. Abplatzungsversuche (Spalling Tests). *Technical University of Braunshweig (internal report)*, Braunshweig, Germany, 1965, 59-66.

[12] Dougill J.W. The Effects of High Temperature on the Strength of Concrete with Reference to Thermal Spalling. PhD Thesis, *King's College London*, UK, 1971, 502 pp.

[13] Chandra S., Berntsson L., and Andergerg Y. Some Effects of Polymer Addition on the Fire Resistance of Concrete. *Cement and Concrete Research*, 1980, 10 (3), 367-375.

[14] Copier W.J. The Spalling of Normal Weight and Lightweight Concrete on Exposure to Fire. *American Concrete Institute Special Publication on High Strength Concrete: An International (ACI SP-80-7)*, 1983, 219-236.

[15] Chan S.Y.N., Peng G.F., and Anson M. Fire Behavior of High-Performance Concrete Made with Silica Fume at Various Moisture Contents. *ACI Materials Journal*, 1999, 96 (3), 405-409.

638 [16] Bailey C.G. Holistic Behaviour of Concrete Buildings in Fire. Proceedings of the
639 *Institution of Civil Engineering - Structures and Buildings*, 2002, 152 (3), 199-212.

640 [17] Hertz K.D. and Sørensen L.S. Test Method for Spalling of Fire Exposed Concrete. *Fire*
641 *Safety Journal*, 2005, 40 (5), 466-476.

642 [18] Jansson R. and Boström L. The Influence of Pressure in the Pore System on Fire
643 Spalling of Concrete. *Fire Technology*, 2010, 46 (1), 271-230.

644 [19] Connolly R.J. The Spalling of Concrete in Fires. PhD Thesis, *Aston University*, UK,
645 1995, 295 pp.

646 [20] Ahmed G.N. and Hurst J.P. Modelling Pore Pressure, Moisture, and Temperature in
647 High-Strength Concrete Columns Exposed to Fire. *Fire Technology*, 1999, 35 (3), 232-
648 262.

649 [21] Shamalta M., Breunese A., Peelen W., and Fellinger J. Numerical Modelling and
650 Experimental Assessment of Concrete Spalling in Fire. *Heron Journal*, 2005, 50 (4),
651 303-319.

652 [22] Arup Fire. Fire Resistance of Concrete Enclosure – Work Package 3 and 4 (Rev A).
653 *Elaborated for the Nuclear Safety Directorate of the Health and Safety Executive*,
654 London, UK, 2005, 52 pp.

655 [23] Deeny S., Stratford T., Dhakal R.P., Moss P.J., and Buchanan A.H. Spalling of
656 Concrete: Implications for Structural Performance in Fire. Proceedings of the
657 *International Conference Applications of Structural Fire Engineering*, Prague, Czech
658 Republic, 2008, 202-207.

659 [24] Bilodeau A., Kodur V.K.R., and Hoff G.C. Optimization of the Type and Amount of
660 Polypropylene Fibres for Preventing the Spalling of Lightweight Concrete Subjected to
661 Hydrocarbon Fire. *Cement & Concrete Composites*, 2004, 26 (2), 163-174.

662 [25] Jansson R. Fire Spalling of Concrete – Theoretical and Experimental Studies. PhD
663 Thesis, *KTH Royal Institute of Technology*, Stockholm, Sweden, 2013, 154 pp.

664 [26] Khoury G.A. Polypropylene Fibres in Heated Concrete – Part 2: Pressure Relief
665 Mechanisms and Modelling Criteria. *Magazine of Concrete Research*, 2008, 60 (3),
666 189-204.

667 [27] Kumar R., Goel P., and Mathur R. Suitability of Concrete Reinforced with Synthetic
668 Fiber for the Construction of Pavements. Proceedings of the *3rd International*
669 *Conference on Sustainable Construction Materials and Technologies*, Kyoto, Japan,
670 2013, 8 pp.

671 [28] Heo Y.S., Sanjayan J.G., Han C.G., and Han M.C. Critical Parameters of Nylon and
672 other Fibres for Spalling Protection of High Strength Concrete in Fire. *Materials and*
673 *Structures*, 2011, 44 (3), 599-610.

674 [29] Eurocode: Design of Concrete Structures – Parts 1-2: General rules – Structural Fire
675 Design (EN 1992-1-2). *European Committee for Standardization*, Brussels, Belgium,
676 2004, 100 pp.

677 [30] CCAA. Fire Safety of Concrete Buildings. *Cement Concrete & Aggregates Australia*
678 *(CCAA)*, 2013, 33 pp.

679 [31] Heo Y.S., Sanjayan J.G., Han C.G., and Han M.C. Relationship between inter-
680 aggregate spacing and the optimum fiber length for spalling protection of concrete in
681 fire. *Cement and Concrete Research*, 2012, 43 (3) 549-557.

682 [32] Terrasi G.P., Bisby L., Barbezat M., Affolter C., and Hugi, E. Fire Behavior of Thin
683 CFRP Pretensioned High-Strength Concrete Slabs. *Journal of Composites for*
684 *Construction*, 2012, 16 (4), 381–394.

685 [33] Maluk C., Bisby L., Krajcovic M., and Torero J.L. The Heat-Transfer Rate Inducing
686 System (H-TRIS) Test Method. *Fire Safety Journal*, 2015. (sent to editor)

687 [34] Robertson A.F. Development of an improved radiant heat source for fire testing, *Fire*
688 *and Materials*, 1982, 6 (2), 68-71.

689 [35] Eurocode: Design of Concrete Structures – Parts 1-1: General Rules and Rules for
690 Buildings (EN 1992-1-1:2004). *European Committee for Standardization*, Brussels,
691 Belgium, 2004, 230 pp.

692 [36] Eurocode: Testing Fresh Concrete – Part 8: Self-compacting Concrete – Slump-Flow
693 Test (EN 12350-8:2010). *European Committee for Standardization*, Brussels, Belgium,
694 2010, 14 pp.

695 [37] Zeiml M., Lackner R., and Mang H.A. Experimental Insight into Spalling Behavior of
696 Concrete Tunnel Linings Under Fire Loading. *Acta Geotechnica*, 2008, 3 (4), 295-308.

697 [38] Maluk C., Bisby L., and Terrasi G.P. Effects of polypropylene fibre type on occurence
698 of heat-induced concrete spalling. Proceedings of the *3rd International RILEM*
699 *Workshop on Concrete Spalling due to Fire Exposure*, Paris, France, 2013, 51-58.